

Fabrication of drug-loaded polymer microparticles with arbitrary geometries using a piezoelectric inkjet printing system

Byung Kook Lee^{a,b,1}, Yeon Hee Yun^{a,b,1}, Ji Suk Choi^{a,b}, Young Chan Choi^{a,b}, Jae Dong Kim^{a,b}, Yong Woo Cho^{a,b,*}

^a Department of Chemical Engineering, Hanyang University, Ansan, Gyeonggi-do 426-791, Republic of Korea

^b Department of Bionanotechnology, Hanyang University, Ansan, Gyeonggi-do 426-791, Republic of Korea

ARTICLE INFO

Article history:

Received 11 November 2011

Received in revised form 10 January 2012

Accepted 9 February 2012

Available online 15 February 2012

Keywords:

Inkjet printing

Microparticles

Geometry

Drug release

In vitro cytotoxicity

ABSTRACT

Carrier geometry is a key parameter of drug delivery systems and has significant impact on the drug release rate and interaction with cells and tissues. Here we present a piezoelectric inkjet printing system as a simple and convenient approach for fabrication of drug-loaded polymer microparticles with well-defined and controlled shapes. The physical properties of paclitaxel (PTX)-loaded poly(lactic-co-glycolic acid) (PLGA) inks, such as volatility, viscosity and surface tension, were optimized for piezoelectric inkjet printing, and PTX-loaded PLGA microparticles were fabricated with various geometries, such as circles, grids, honeycombs, and rings. The resulting microparticles with 10% (w/w) PTX exhibited a fairly homogeneous shape and size. The microparticle fabrication by piezoelectric inkjet printing was precise, reproducible, and highly favorable for mass production. The microparticles exhibited a biphasic release profile with an initial burst due to diffusion and a subsequent, slow second phase due to degradation of PLGA. The release rate was dependent on the geometry, mainly the surface area, with a descending rate order of honeycomb > grid, ring > circle. The PTX-loaded microparticles showed a comparable activity in inhibiting the growth of HeLa cells. Our results demonstrate that a piezoelectric inkjet printing system would provide a new approach for large-scale manufacturing of drug carriers with a desired geometry.

© 2012 Elsevier B.V. All rights reserved.

1. Introduction

Designing polymeric carriers for drug delivery is a topic of great interest. Extensive studies have focused on the optimization of physical design, such as carrier geometry, size and surface modification, to further enhance carrier effectiveness (Varde and Pack, 2004). In particular, the geometry of the drug carrier has been recently demonstrated to have an impact on biological processes, such as vasculature, circulation time, targeting efficiency, phagocytosis, endocytosis and subsequent intracellular transport for therapeutic delivery (Decuzzi et al., 2010). Carrier geometry is indeed a key design parameter of drug delivery systems.

Non-spherical shapes including ellipsoids, discs, cubes, cylinders, doughnut, hemispheres, cones, needles, and bio-mimicking shapes have been designed using a variety of fabrication techniques (Doshi and Mitragotri, 2010; Geng et al., 2007; Sundy and Danckwerts, 2004). A number of conventional methods such as

spray drying, emulsion/solvent evaporation, and phase separation, have been used for manufacturing drug carriers (Jain, 2000; Nykamp et al., 2002; Rawat and Burgess, 2011). However, these methods are limited to production of relatively wide size distribution and shape. Recently, lithographic fabrication techniques have been developed for nano/micro-carriers with a well-defined shape, homogeneous size and structure. Despite their success in producing homogeneous micro/nano-structures, lithographic fabrication techniques are not readily applicable because of hindrances, such as complicated procedures and high cost associated with raw materials, facilities, and processing (Ahmed et al., 2001, 2002). Thus, simple and convenient processes are desired for large-scale manufacturing of drug carriers with intricate and complex designs.

Herein, we used a direct-writing, drop-on-demand, piezoelectric inkjet printing system for fabrication of drug carriers with different geometries. Inkjet printing has recently been emerging as an attractive manufacturing alternative in a broad range of biomedical devices including cell-based assay systems, biosensors, biochips and tissue engineering scaffolds (Kim et al., 2010; Roth et al., 2004; Sumerel et al., 2006; Yun et al., 2011). Inkjet printing can create arbitrary and complex polymer architectures, and patterns are directly created by depositing a minute quantity of material at desired locations. Moreover, it can dramatically reduce the manufacturing cost, material waste, and manufacturing

* Corresponding author at: Department of Chemical Engineering, Hanyang University, Ansan, Gyeonggi-do 426-791, Republic of Korea. Tel.: +82 31 400 5279; fax: +82 31 696 5279.

E-mail address: ywcho7@hanyang.ac.kr (Y.W. Cho).

¹ Both authors contributed equally to this work.

process steps (Yu et al., 2009; Yun et al., 2009; Zheng et al., 2011). In the present study, we successfully fabricated paclitaxel (PTX)-loaded poly(lactic-co-glycolic acid) (PLGA) microparticles with a wide variety of geometries, such as circles, grids, honeycombs, and rings, via piezoelectric inkjet printing. The effect of the drug carrier geometry on the drug release behavior was investigated.

2. Materials and methods

2.1. Materials

PLGA (M_w 27,000, LA:GA = 70:30) was supplied by KITECH (Ansan, Gyeonggi, Korea). Paclitaxel (PTX) was obtained from Samyang Genex (Daejeon, Korea). Fluorescein 5-isothiocyanate (FITC) and phosphate buffered saline (PBS, pH 7.4) were purchased from Sigma-Aldrich (St. Louis, MO). Penicillin-streptomycin (P/S), trypsin-EDTA, fetal bovine serum (FBS) and Dulbecco's Modified Eagle's Medium (DMEM) were purchased from PAA Laboratories GmbH (Pasching, Austria). Tween 80 was purchased from Tokyo Chemical Industry (Toshima, Tokyo, Japan). N,N-dimethylacetamide (DMAc) was purchased from Dae Jung Chemical & Metals (Siheung, Gyeonggi, Korea). Acetonitrile (AcN) was purchased from Duksan Pure Chemicals (Ansan, Gyeonggi, Korea). A human cervical cancer (HeLa) cell line was provided by Korean Cell Line Bank® (Seoul, Korea). The premix WST-1 assay was purchased from TAKARA Bio (Otsu, Shiga, Japan). All chemicals were of analytical grade and used as received.

2.2. Preparation and characterization of PTX-loaded PLGA inks

PLGA inks (10%, w/v) were prepared by dissolving PLGA in DMAc. PLGA solutions were stirred for 3 h at 35 °C, and were passed through a 0.2-μm syringe filter to eliminate insoluble particles. Subsequently, 1% (w/v) PTX was added to the PLGA solution and stirred until homogenously mixed. The viscosity of the ink was measured at 25 °C with a digital viscometer (LVDV II+ Pro CP, Brookfield Engineering Laboratories, Middleboro, MA). A surface tension analyzer (CAHN Instruments, Cerritos, CA) was used to measure its surface tension.

2.3. Piezoelectric inkjet printing

Printing was conducted on a piezoelectric inkjet printer (Dimatix, Santa Clara, CA) in a clean bench. Each glass slide (25 mm × 75 mm) was cleaned in a stream of nitrogen gas. A glass slide was placed inside the chamber of a Radio Frequency (RF) plasma deposition system (SNTEK, Gimpo, Korea) and the surface of glass slide was treated by oxygen gas plasma at room temperature. The PLGA ink containing PTX was loaded into a cartridge and then printed on the prepared glass slide. Patterns with different geometries (circles, grids, honeycombs and rings) were designed using Photoshop CS (Adobe Systems, San Jose, CA). The plate and head temperature of the cartridge were set to 28–31 °C. The firing voltage and frequency were 20–23 V and 5 kHz, respectively. After printing, the patterns were dried for 2 h in a drying oven.

2.4. Particle morphology analysis

After printing, the width and height of the patterns were analyzed using a high accuracy non-contact surface profiler (Nano System, Daejeon, Korea). To visualize the morphology, a small amount of FITC was added to PTX-loaded PLGA inks, which were patterned on the glass slide and observed by a fluorescence microscope (IX81, Olympus, Tokyo, Japan) equipped with a digital camera.

2.5. In vitro PTX release profile

PTX-loaded PLGA microparticles with different geometries were placed into 15 mL conical tubes and 5 mL of PBS/Tween 80 (0.1%, v/v) medium was transferred into each tube. The tubes were kept in an orbital shaker maintained at 37 °C with constant agitation (50 rpm). At appropriate time intervals, the release medium was withdrawn from the tube and replaced with fresh medium. The collected samples were transferred into 15 mL conical tubes and stored in a refrigerator. Sampling of the medium was continued for 6 d.

Each sample was analyzed using HPLC (ÄKTAexplorer™, GE Healthcare, Waukesha, WI) with an UV detector set at 205 nm. A Symmetry® C18 (4.6 mm × 150 mm, Milford, MA) analytical column was used at a flow rate of 1.0 mL/min. A mixture of acetonitrile and water (50:50, v/v) was used as a mobile phase and the injection volume was 20 μL. The amounts of PTX in samples were calculated from a reference standard calibration curve. All measurements were carried out in triplicate.

The morphology of degraded PLGA microparticles was examined by scanning electron microscopy (SEM; VEGA-II SBH, TESCAN, Brno, Czech Republic). Samples were observed after coating with platinum by sputtering at an acceleration voltage of 15 kV.

2.6. Release profiles

Release kinetics were analyzed using the Higuchi Eq. (1) in order to clarify the PTX release mechanism from the PLGA microparticles (Higuchi, 1961; Paul, 2011):

$$Q = kt^{1/2} \quad (1)$$

where Q is the fraction of drug released at release time t and k is the release constant. The correlation between experimental data and the Higuchi model results was evaluated using the correlation coefficient r^2 .

2.7. In vitro cytotoxicity

A cell cytotoxicity assay was performed using a WST-1-based colorimetric assay, which relies upon the ability of living cells to reduce a tetrazolium salt into a soluble colored formazan product. HeLa cells were routinely cultured in DMEM supplemented with 10% FBS and 1% P/S at 37 °C under 5% CO₂ to reach a sub-confluent state. Cells were harvested by trypsin-EDTA treatment, resuspended in medium, and seeded on a 24-well plate at a density of 1×10^4 cells/well. The cells were allowed to attach to the plate bottom for 24 h and unattached cells were removed by rinsing with PBS. The PTX-loaded PLGA microparticles were directly added to cell culture medium with different concentrations of PTX and the cells were then incubated for 48 h. The WST-1 reagent was added to each well containing cells, and PLGA microparticles and the plates were incubated at 37 °C for 1 h under 5% CO₂. After gentle pipetting, the 100 μL solution was transferred to a 96-well plate. The optical density was then measured at 440 nm using a microplate spectrophotometer (PowerWave XS, Bio-Tek Instruments, Winooski, VT). These experiments were performed in triplicate.

2.8. Statistical analysis

Experimental data was expressed as means ± standard deviation (SD). Student's two tailed *t*-test with SPSS 17.0 statistical software (SPSS, Chicago, IL) was used for comparison, and statistical significance was accepted at $p < 0.05$.

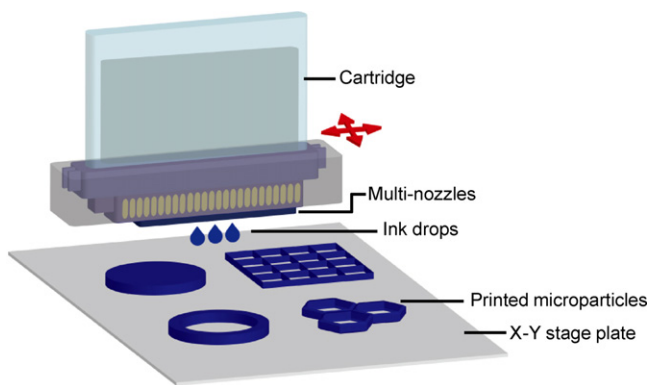


Fig. 1. Schematic representation of the piezoelectric inkjet printing system for fabrication of PTX-loaded PLGA microparticles.

3. Results and discussion

3.1. Fabrication of PTX-loaded PLGA microparticles by piezoelectric inkjet printing

Fig. 1 schematically represents a diagram for fabrication of drug-loaded microparticles by piezoelectric inkjet printing. The inkjet printer consists of a cartridge, a printer head with multi-nozzles, a print head driver, an X-Y stage plate, and a host computer with software. First of all, the physical properties of the ink, such as solubility, volatility, viscosity, and surface tension, were optimized for inkjet printability (**Table 1**). PLGA, a well-known biocompatible and biodegradable polymer was chosen as a matrix material. DMAc, a non-volatile solvent (boiling point 165 °C) was used in order to prevent nozzle clogging. When a volatile solvent, such as chloroform (boiling point 61.2 °C), was used as a solvent for PLGA, nozzle clogging occurred frequently, especially when the nozzle

Table 1
Components and basic properties of the ink.

Ink components	
Solvent	DMAc
PLGA	100 mg/mL
PTX	10 mg/mL
Ink properties (at 25 °C)	
Viscosity	5.99 cps
Surface tension	35.40 mN/m

was undisturbed. The use of a non-volatile solvent significantly relieved the clogging phenomenon.

Ink viscosity and surface tension should also be controlled. Ink viscosity should be low, typically below 20 cps, because the jetting force generated by a piezoelectric inkjet printer is limited (*Sumerel et al., 2006*). The surface tension should be 30–70 mN/m, high enough to prevent dripping of the ink from the nozzle and low enough to allow spreading over the substrate (*Calvert, 2001*). The viscosity of the ink containing 10% (w/v) PLGA and 1% (w/v) PTX was 5.99 cps, low enough for stable jetting and the surface tension was 35.4 mN/m, which was higher than the bottom limit (30 mN/m). The PLGA/PTX/DMAc ink showed appropriate inkjet printability and the ink droplets were continuously and stably ejected from the nozzles. Prior to inkjet printing, the surface of a glass slide was treated with oxygen gas plasma for surface uniformity. For clear visualization, a small amount of FITC was added to the PLGA/PTX/DMAc ink.

Microparticles of four different shapes (circles, grids, honeycombs, and rings) were printed on the plasma-treated glass slide and observed using a fluorescence microscope (**Fig. 2**). The lateral sizes, surface areas and volumes measured by a high accuracy non-contact surface profiler are listed in **Table 2**. The drug loading amount in the microparticles was approximately 10% (w/w). The resulting microparticles had a fairly homogeneous shape and size. Microparticle fabrication by piezoelectric inkjet printing was

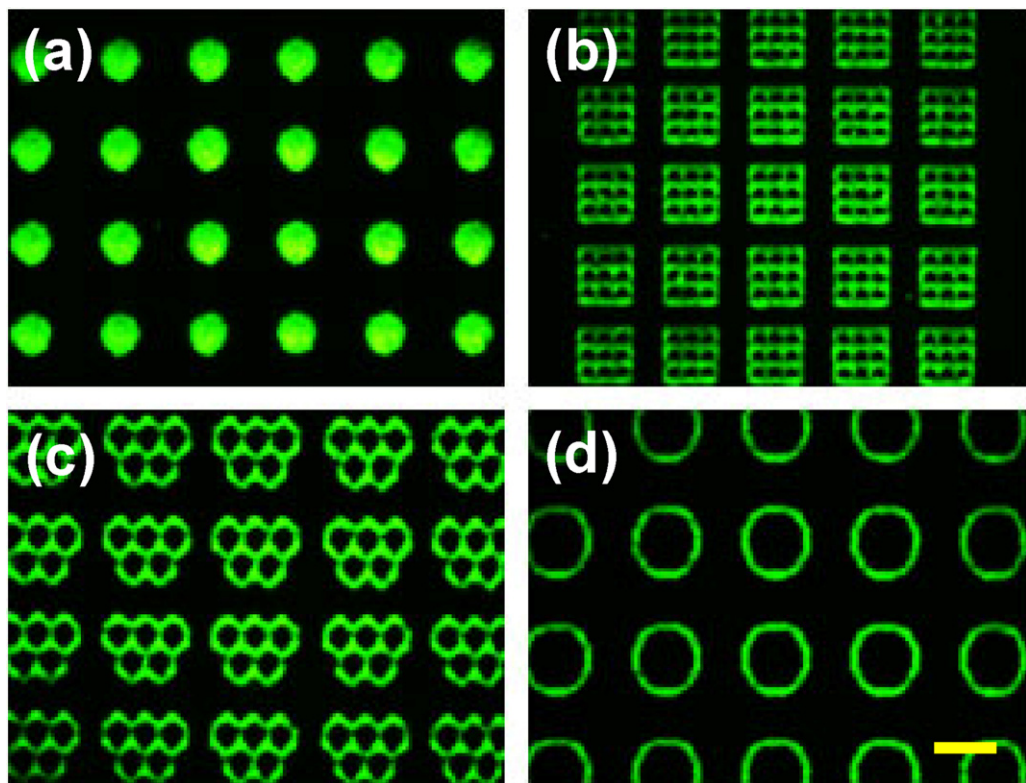


Fig. 2. Fluorescence micrographs of PTX-loaded PLGA microparticles with different geometries. (a) circle, (b) grid, (c) honeycomb, (d) ring. Scale bar represents 500 μm.

Table 2

Geometries and surface properties of PLGA microparticles.

Shape	PTX loading amount (μg)	Weight (μg)	Height (μm)	Volume (μm^3)	Total surface area (μm^2)	Relative surface area
Circle	0.34	6.5	28	3,357,288	235,123	1.00
Grid	0.34	6.5	25	3,010,000	398,800	1.69
Honeycomb	0.32	6.0	23	3,378,033	579,740	2.46
Ring	0.34	6.5	25	3,477,864	367,405	1.56

quite precise, reproducible, and favorable to mass production (e.g., approximately 120,000 circle-shaped microparticles with 350 μm diameter on a 210 mm \times 297 mm substrate at a time). In addition, the inkjet-printed microparticles were easily detached from the substrate with aqueous media, such as water, phosphate buffer or culture medium, thus it can be handled readily for *in vitro* drug release tests and cell-based tests.

3.2. PTX release from microparticles

Fig. 3 shows PTX release profiles from PLGA microparticles with different geometries. The PTX release experiments were performed in PBS containing 0.1% (v/v) Tween 80 because PTX is sparingly soluble in water. The PTX release kinetics exhibited a biphasic pattern characterized by a fast initial release during the first day, followed by slower and continuous release for 6 d. The honeycomb-shaped microparticles released almost all of the drug in 6 d, while grid- and ring-shaped microparticles released approximately 80%. The release rate of circle-shaped microparticles was the slowest, resulting in a total release approximately 60% for 6 d. The morphology change of the PTX-loaded PLGA microparticles during the drug release experiment was monitored by SEM, as shown in Fig. 4. The PLGA microparticles degraded from the surfaces, became gradually wrinkled, and lost the shape integrity.

The geometry of the polymer microparticles is an important factor for modulation of the degradation rate, stability and drug release profile. Water molecules penetrate into particles, and degradation of particles is inversely proportional to the surface area and the dimension (Simone et al., 2008; Varde and Pack, 2004). Therefore, changing the surface area of particles according to different geometries can significantly impact the degradation rate, leading to different drug release rates. In this study, the descending order of the relative surface area was honeycomb > grid > ring > circle, indicating that microparticles with complex structures and inner holes had large surface areas. At the initial stage, all the release profiles of PTX showed a burst effect. The initial burst could be attributed to non-encapsulated PTX molecules on the surface or PTX molecules close to the surface easy accessible by hydration (Fredenberg et al., 2011). After the initial burst, PTX was released slowly and continuously through gradual degradation and hydration of the microparticles. The honeycomb-shaped microparticles showed the fastest release rate (approximately 100%) for 6 d, while the circle-shaped one showed the slowest (approximately 60%). The release rate was dependent on the morphology, mainly the surface area, with a descending order of honeycomb > grid, ring > circle.

A mathematical model by Higuchi following Eq. (1) was used for the diffusional release of PTX from the PLGA matrix. The release profiles of microparticles appeared to have a good correlation with the Higuchi model (Fig. 3(c) and Table 3). The experimental values fit the theoretical curve ($r^2 > 0.98$). Consequently, the main PTX

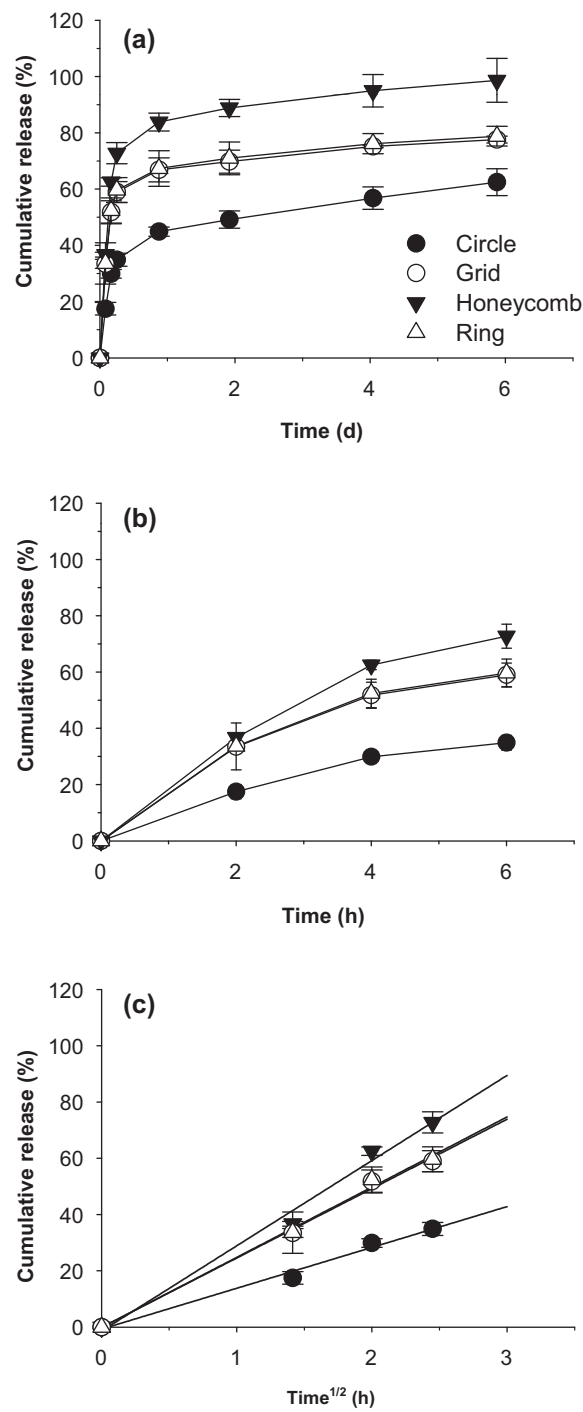


Fig. 3. Release profiles in cumulative percentage of PTX released from PLGA microparticles with four different geometries (● circle, ○ grid, ▼ honeycomb, and △ ring) in PBS containing 0.1% (v/v) Tween 80 at 37°C for (a) 6 d (b) 6 h and (c) the cumulative release (%) as a function of the square root of time. Data are shown as means \pm standard deviations ($n = 3$).

Table 3Apparent release rate constants (k) and correlation coefficients (r^2) of PTX-loaded PLGA microcarriers with different shapes.

Shape	Circle	Grid	Honeycomb	Ring
k	14.51	24.66	30.28	24.95
r^2	0.99	0.99	0.99	0.98

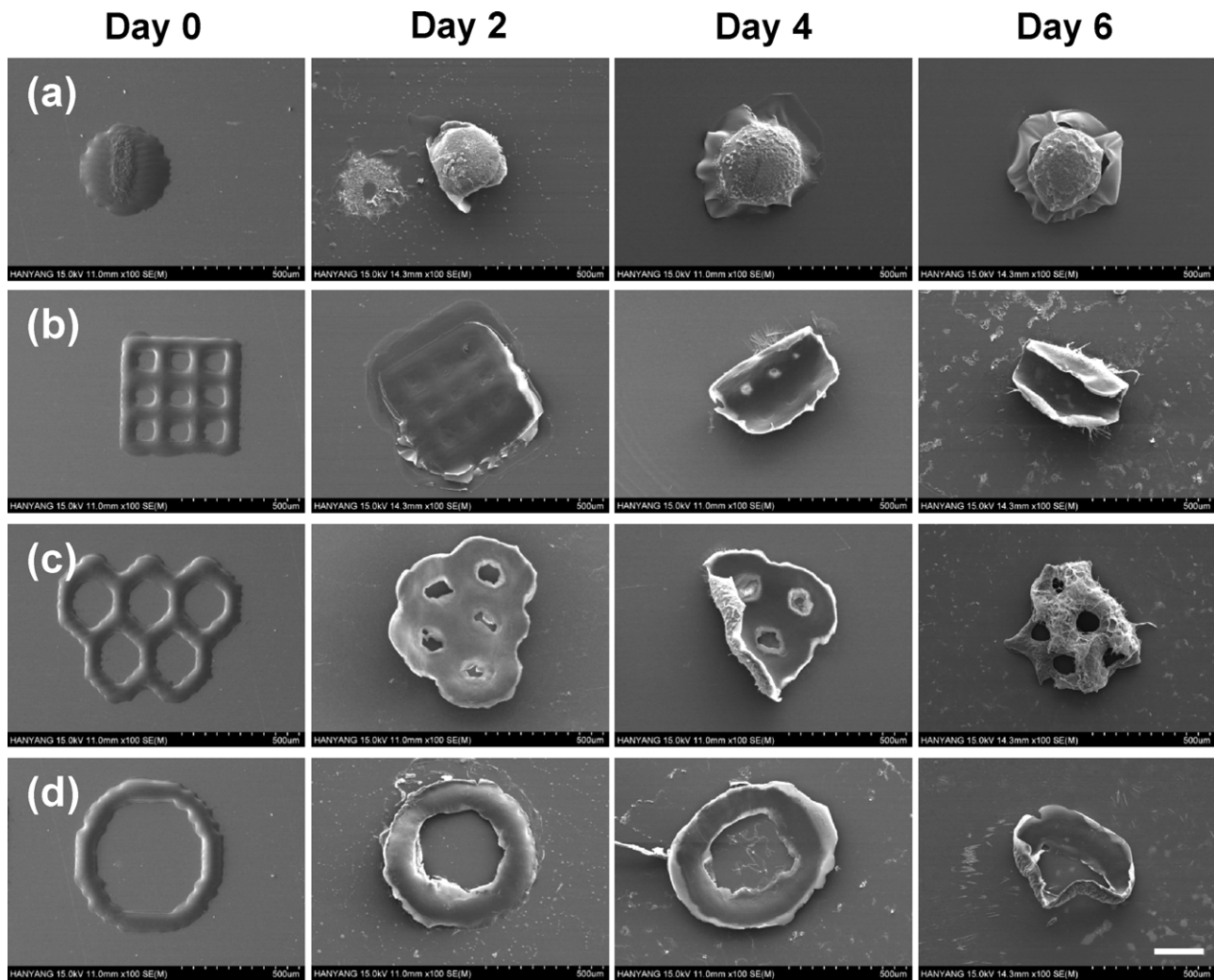


Fig. 4. SEM images of PLGA microparticles degraded in PBS containing 0.1% (v/v) Tween 80 for 6 d. (a) circle (b) grid (c) honeycomb (d) ring. Scale bar represents 200 μ m.

release mechanism could be diffusion through erosion from the outside edge of the PLGA microparticles.

3.3. In vitro cytotoxicity

To assess the cytotoxic effect on the cells of PTX-loaded PLGA microparticles, the circle-shaped microparticles, which showed a sustained release profile, was chosen and the *in vitro* cytotoxicity was evaluated by the WST-1 assay using the HeLa cell line, as shown in Fig. 5. PTX, a well-known anticancer agent has shown

significant anti-tumor activity against various tumors such as breast and ovarian cancers (Danhier et al., 2009). The PTX-loaded microparticles were used at PTX concentrations ranging from 340 nM to 3400 nM. The cytotoxicity increased with the PTX dose and incubation time. Just one PTX-loaded microparticle (PTX 340 nM) greatly reduced the cell viability. When 10 PTX-loaded microparticles (3400 nM) were added, the cell viability was reduced to less than 10%. The PTX-free microparticles did not induce the cytotoxicity to the HeLa cells during the test period. The PTX dosage could be readily

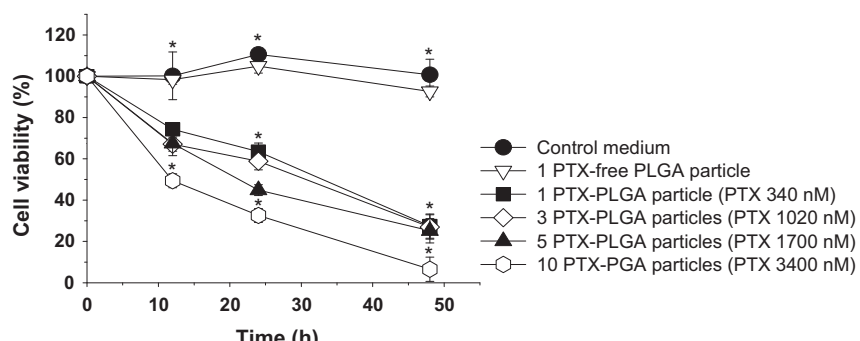


Fig. 5. *In vitro* cytotoxicity of PTX-loaded PLGA microparticles with a circle shape against human cervical cancer (HeLa) cells. Cell viability was assessed by the WST-1 assay. Data are shown as means \pm standard deviations ($n=3$) with significance at $^*p < 0.05$.

manipulated through simple control of the number of the drug-loaded microparticles or the drug-loading amount in the ink formulation.

Drug carrier geometry is one of essential properties and has an important role in mitigating cellular responses (Mitragotri and Lahann, 2009). Many studies have pointed to the role of carrier geometry in drug delivery. Drug carriers of different geometries have been shown to perform different delivery functions (Doshi and Mitragotri, 2009). Traditionally, drug delivery carriers prepared by emulsion methods have heterogeneous spherical shape and may produce undesirable variation in the rate of degradation, drug stability and drug release kinetics (Xu et al., 2009). Therefore, fabrication of non-spherical carriers with arbitrary geometries has been challenging not only for fundamental studies of the influence of the shape on their biological behavior, but also for new therapeutic applications of drug-loaded microparticles. Indeed, several techniques have been developed for fabricating drug carriers with diverse shapes at nano- and micro-scales (Champion et al., 2007). These techniques include soft lithography, microfluidics and self-assembly. They produced drug carriers with a highly uniform size and well-defined micro/nano-structures and showed better shape accuracy than inkjet printing systems (Dendukuri et al., 2005, 2006; Guan et al., 2006; Manoharan et al., 2003; Yin et al., 2001). Nonetheless, particularly in terms of engineering aspects, inkjet printing has many appealing advantages, such as simplicity, arbitrary geometries, low usage of raw materials, low cost and flexibility in shape change. In this study, we explored the feasibility of inkjet printing systems for fabrication of drug-loaded microparticles with diverse shapes. We hope that this approach will generate further interest in the precise control of morphology of drug carriers and trigger detailed investigation of their morphology-dependent drug release and biological properties.

4. Conclusions

Intricate microparticles with various geometries were successfully created using piezoelectric inkjet printing. PTX-loaded PLGA microparticles with different geometries exhibited different drug release rates mainly due to different surface areas. *In vitro* cytotoxicity tests against the HeLa cell line showed a cytotoxic effect of PTX released from microparticles. The fabrication technique of microparticles using inkjet printing systems would provide platforms for studying and developing novel drug delivery carriers, offering new approaches for preparing drug carriers involving complex design features with desired release profiles.

Acknowledgments

This work was supported by a Korea Science and Engineering Foundation (KOSEF) grant funded by the Korea government (MEST) (Grant No. R11-2008-044-02001-0 and R01-2008-000-20460-0). This work was also supported by the Human Resources Development of the Korea Institute of Energy Technology Evaluation and Planning (Grant No. 20104010100620) grant funded by the Ministry of Knowledge Economy, Republic of Korea.

References

Ahmed, A., Bonner, C., Desai, T.A., 2001. Bioadhesive microdevices for drug delivery: a feasibility study. *Biomed. Microdevices* 3, 89–96.

Ahmed, A., Bonner, C., Desai, T.A., 2002. Bioadhesive microdevices with multiple reservoirs: a new platform for oral drug delivery. *J. Control. Release* 81, 291–306.

Calvert, P., 2001. Inkjet printing for materials and devices. *Chem. Mater.* 13, 3299–3305.

Champion, J.A., Katare, Y.K., Mitragotri, S., 2007. Particle shape: a new design parameter for micro- and nanoscale drug delivery carriers. *J. Control. Release* 121, 3–9.

Danhier, F., Lecouturier, N., Vroman, B., Jérôme, C., Marchand-Brynaert, J., Feron, O., Préat, V., 2009. Paclitaxel-loaded PEGylated PLGA-based nanoparticles: *in vitro* and *in vivo* evaluation. *J. Control. Release* 133, 11–17.

Decuzzi, P., Godin, B., Tanaka, T., Lee, S.-Y., Chiappini, C., Liu, X., Ferrari, M., 2010. Size and shape effects in the biodistribution of intravascularly injected particles. *J. Control. Release* 141, 320–327.

Dendukuri, D., Pregibon, D.C., Collins, J., Hatton, T.A., Doyle, P.S., 2006. Continuous-flow lithography for high-throughput microparticle synthesis. *Nat. Mater.* 5, 365–369.

Dendukuri, D., Tsoi, K., Hatton, T.A., Doyle, P.S., 2005. Controlled synthesis of non-spherical microparticles using microfluidics. *Langmuir* 21, 2113–2116.

Doshi, N., Mitragotri, S., 2009. Designer biomaterials for nanomedicine. *Adv. Funct. Mater.* 19, 3843–3854.

Doshi, N., Mitragotri, S., 2010. Needle-shaped polymeric particles induce transient disruption of cell membranes. *J. R. Soc. Interface* 7, S403–S410.

Fredenberg, S., Wahlgren, M., Reslow, M., Axelsson, A., 2011. The mechanisms of drug release in poly(lactic-co-glycolic acid)-based drug delivery systems—a review. *Int. J. Pharm.* 415, 34–52.

Geng, Y., Dalheimer, P., Cai, S., Tsai, R., Tewari, M., Minko, T., Discher, D.E., 2007. Shape effects of filaments versus spherical particles in flow and drug delivery. *Nat. Nanotechnol.* 2, 249–255.

Guan, J., Ferrell, N., Lee, L.J., Hansford, D.J., 2006. Fabrication of polymeric microparticles for drug delivery by soft lithography. *Biomaterials* 27, 4034–4041.

Higuchi, T., 1961. Rate of release of medicaments from ointment bases containing drugs in suspension. *J. Pharm. Sci.* 50, 874–875.

Jain, R.A., 2000. The manufacturing techniques of various drug loaded biodegradable poly(lactide-co-glycolide) (PLGA) devices. *Biomaterials* 21, 2475–2490.

Kim, J.D., Choi, J.S., Kim, B.S., Choi, Y.C., Cho, Y.W., 2010. Piezoelectric inkjet printing of polymers: stem cell patterning on polymer substrates. *Polymer* 51, 2147–2154.

Manoharan, V.N., Elsesser, M.T., Pine, D.J., 2003. Dense packing and symmetry in small clusters of microspheres. *Science* 301, 483–487.

Mitragotri, S., Lahann, J., 2009. Physical approaches to biomaterial design. *Nat. Mater.* 8, 15–23.

Nykamp, G., Carstensen, U., Müller, B.W., 2002. Jet milling—a new technique for microparticle preparation. *Int. J. Pharm.* 242, 79–86.

Paul, D.R., 2011. Elaborations on the Higuchi model for drug delivery. *Int. J. Pharm.* 418, 13–17.

Rawat, A., Burgess, D.J., 2011. Effect of physical ageing on the performance of dexamethasone loaded PLGA microspheres. *Int. J. Pharm.* 415, 164–168.

Roth, E.A., Xu, T., Das, M., Gregory, C., Hickman, J.J., Boland, T., 2004. Inkjet printing for high-throughput cell patterning. *Biomaterials* 25, 3707–3715.

Simone, E.A., Dziubla, T.D., Muzykantov, V.R., 2008. Polymeric carriers: role of geometry in drug delivery. *Expert Opin. Drug Deliv.* 5, 1283–1300.

Sumerel, J., Lewis, J., Doraiswamy, A., Deravi, L.F., Sewell, S.L., Gerdon, A.E., Wright, D.W., Narayan, R.J., 2006. Piezoelectric ink jet processing of materials for medical and biological applications. *Biotechnol. J.* 1, 976–987.

Sundy, E., Danckwerts, M.P., 2004. A novel compression-coated doughnut-shaped tablet design for zero-order sustained release. *Eur. J. Pharm. Sci.* 22, 477–485.

Varde, N.K., Pack, D.W., 2004. Microspheres for controlled release drug delivery. *Expert Opin. Biol. Ther.* 4, 35–51.

Xu, Q., Hashimoto, M., Dang, T.T., Hoare, T., Kohane, D.S., Whitesides, G.M., Langer, R., Anderson, D.G., 2009. Preparation of monodisperse biodegradable polymer microparticles using a microfluidic flow-focusing device for controlled drug delivery. *Small* 5, 1575–1581.

Yin, Y., Lu, Y., Gates, B., Xia, Y., 2001. Template-assisted self-assembly: a practical route to complex aggregates of monodispersed colloids with well-defined sizes, shapes, and structures. *J. Am. Chem. Soc.* 123, 8718–8729.

Yu, D.-G., Branford-White, C., Ma, Z.-H., Zhu, L.-M., Li, X.-Y., Yang, X.-L., 2009. Novel drug delivery devices for providing linear release profiles fabricated by 3DP. *Int. J. Pharm.* 370, 160–166.

Yun, Y.H., Kim, J.D., Lee, B.K., Cho, Y.W., 2009. Polymer inkjet printing: construction of three-dimensional structures at micro-scale by repeated lamination. *Macromol. Res.* 17, 197–202.

Yun, Y.H., Lee, B.K., Choi, J.S., Kim, S., Yoo, B., Kim, Y.S., Park, K., Cho, Y.W., 2011. A glucose sensor fabricated by piezoelectric inkjet printing of conducting polymers and bienzymes. *Anal. Sci.* 27, 375–379.

Zheng, Q., Lu, J., Chen, H., Huang, L., Cai, J., Xu, Z., 2011. Application of inkjet printing technique for biological material delivery and antimicrobial assays. *Anal. Biochem.* 410, 171–176.